PHYSICAL REVIEW B VOLUME 25, NUMBER 2 15 JANUARY 1982

# Mass- and charge-density modulation of graphite in potassium-graphite intercalates

M. Mori,* S. C. Moss, and Y. M. Jan
*Department of Physics, University of Houston, Houston, Texas 77004*

H. Zabel
*Department of Physics, University of Illinois at Urbana-Champaign, Urbana, Illinois 61801*
(Received 8 August 1980: revised manuscript received 22 May 1981)

X-ray evidence on a stage-II potassium-graphite crystal indicates that below the upper critical temperature, $T_U \cong 123$ K, the disordered unregistered potassium layers order and rotate with respect to the graphite. We postulate that the alkali ordering is accompanied by both a static displacement and charge-density modulation of the adjacent graphite planes in which the potassium periodicity is impressed. We then make preliminary estimates of these modulation amplitudes. A simple $\vec{k}$-space geometrical argument relates the rotation angle to the alkali ion size in K, Rb, and Cs compounds, and a universal curve is thereby generated which fits well the available data.

## I. INTRODUCTION

From previous x-ray studies of stage-II potassium-intercalated graphite ($C_{24}K$) we know: (a) the high-temperature disordered state shows an $l$-independent scattering[1,2] ($l$ is the reciprocal-lattice index normal to the graphite basal plane; $h$ and $k$ are in the basal plane) characteristic of uncorrelated potassium layers; (b) the two-dimensional (2D) in-plane disorder scattering shows liquidlike behavior,[2,3] similar to the observation of Clarke *et al.*[4] on disordered $C_{24}Cs$, which cannot be fit with a simple lattice-gas model[3] and is indicative of a potassium 2D liquid unregistered with the graphite; (c) at an upper phase transition,[2,5] $T_U \cong 123$ K, the potassium layers order, giving rise to new 3D Bragg peaks whose intensity grows continuously as in a second-order phase transition; above $T_U$ there remains some critical scattering at the reciprocal-lattice points (relpoints) of the low-temperature structure, which is 2D in character; (d) at $T_L \cong 95$ K, a first-order transition occurs,[1,5] associated with a new potassium stacking sequence. At $T_L < T < T_U$, the intercalated potassium stacking is $\alpha\beta\gamma/\alpha\beta\gamma$ with a complete graphite-potassium stacking of $A\alpha AB\beta BC\gamma C\ldots$,etc. It is generally agreed that each potassium layer is always confined by two carbon layers directly over each other.

Relevant x-ray and neutron data from other systems with which these results may be compared include observations on ordering in single-crystal $C_{24}Cs$ (Refs. 4 and 6) and highly oriented pyrolytic graphite[7] (HOPG) and single-crystal[8] $C_{24}Rb$. There are also electron diffraction data[9] on the ordered structures in these three stage-II compounds which show similar effects. (The designation $C_{24}X$ is used interchangeably with stage II; if the intercalation does not result in a registered structure, there is no requirement of exact stoichiometry.) In the most recent of these related studies[4,6–8] (see also Ref. 10 for a review and preliminary announcement of the present findings), it has been noted that the planar ordered alkali lattice is incommensurate with its graphite host and is rotated with respect to the graphite lattice. In addition, in analogy, for example, with rare-gas overlayers on graphite,[11] the diffraction patterns of the ordered stage-II compounds demonstrate a modulation pattern initially attributed[4,7] to the modulation of the alkali layer by the neighboring graphite potential. Difficulties in this interpretation were raised by the present authors as quoted in Ref. 10, and by Yamada *et al.*,[8] and will be discussed presently. It remains true that a complete description of the disordered (liquidlike) state has yet to be given which properly includes graphite-intercalate perturbations. A proper structural analysis of the ordered state, including positions and intensities of the new or extra reflections, has also yet to be made.

 

There seem, however, to be some basic features which should be stressed and which any analysis must ultimately account for. In the first place there appears in the $(hk.0)$ plane of the ordered state a set of 12 alkali spots (6 pairs, each split by a rotational angle $2\theta$ about [10.0] directions). The alkali spots form a ring about the origin of reciprocal space at the same wave vector as the first strong diffuse peak of the liquidlike disordered structure. It is assumed that they develop out of this diffuse peak as indeed seems to be the case.[1-7] Any of these 12 peaks can properly be called an alkali 10.0 reflection (or the $l=0$ extension of a $10.l$ reflection). There are also alkali peaks which may be indexed as 11.0, 20.0, etc., although these peaks fall off rather quickly in intensity. Finally, the entire pattern about the origin in the $(hk.0)$ plane is repeated about each graphite reciprocal-lattice (rel) point. (These aspects are reiterated in the next section because, to our knowledge, this is the first place where they have been discussed in detail other than in Ref. 10.)

Because there appears both a graphite lattice and an ordered alkali lattice incommensurate with it, together with the aforementioned repeat or modulation structure, only a few possibilities for the ordered state exist. One might be the analogy with the rare gases noted above.[7] Another involves a "registered" alkali lattice in which the alkali atoms are moved from their own lattice sites to nearby graphite hexagon centers. This is attractive because it represents an amplitude modulation of the graphite lattice by the alkali atoms, together with displacements of these atoms from their own lattice which would tend to attenuate the alkali Bragg peaks as observed. This model has been proposed by DiCenzo.[12] An extension of this idea, proposed earlier by Yamada *et al.*[8] involves, in addition, in-plane displacements of the graphite atoms as each alkali tries to center itself in a graphite hexagon.

We present here the $C_{24}K$ single-crystal results referred to earlier,[10] together with both a geometrical interpretation and a quantitative estimate of the intensities of the observed modulation satellite peaks in HOPG $C_{24}K$. We also present new HOPG data on ordered $C_{36}K$. The model we develop for the measured intensities is based simply on the modulation of the graphite sandwich by the intercalated potassium lattice which has rotated with respect to it; each graphite hexagon is deformed here to an extent determined by the position of the alkali atom in it. Accompanying this proposed mass-density wave in the graphite is a charge-density wave which tends to pile up the charge donated to the adjacent graphite layers in the region between the potassium ions.

## II. RESULTS AND GEOMETRICAL INTERPRETATION

Figure 1(a) shows an x-ray photograph and its tracing taken at $\sim 100$ K, of a small ($\sim 2.3$ mm$^2$) stage-II potassium-graphite single-crystal flake kindly provided by S. A. Solin and co-workers who prepared it by the 2-bulb Herold method. Careful x-ray scans verified both the stage index (II) and stage purity (instrumentally narrow peaks). (The crystal was in a thin glass tube whose first diffuse maximum unfortunately dominates the low-angle portion of our photograph.) The x-ray source was a 12 kW Rigaku Rotaflex with a Mo anode and point focus geometry. A vertically bent graphite monochromator was used to bring the beam onto the pinhole collimator of our camera, followed by the crystal-in-glass aligned with the flat face approximately normal to the beam. The flat film holder with a beam stop was placed $\sim 7$ cm behind the crystal. The temperature was achieved by flowing cold $N_2$ gas over the sample through a double cone arrangement of Mylar sheets which were warmed with a blower from the outside to prevent ice formation.

We take advantage in Fig. 1(a) of a large mosaic spread about $\vec{c}^* = 2\pi/\vec{c}$ to effectively rotate the crystal onto a Ewald sphere. Using the measured mosaic spread and the radius of the Mo$K\alpha$ sphere, we calculate that effects at least out to the graphite 10.0 position are thus observable. The pattern, however, becomes more distorted with increasing angle due to the flat-film geometry. Distances estimated on the film and its tracing are therefore inaccurate, becoming, in general, increasingly invalid with increasing angle. This effect is additionally complicated by the presence of a large amount of $c$-axis stacking disorder which extends certain reciprocal-lattice points into rods parallel to $\vec{c}^*$.[1,5]

The tracing in Fig. 1(a) shows the following diffraction features summarized above: (a) A sixfold distribution of split spots about the origin where the spot splitting, $\theta$, is about $7-7.5°$ off the graphite [10.0] direction. (b) The reproduction of this pattern of six pairs of split spots about each graphite { 10.0 } relpoint. (c) The extension of a part of the single-crystal pattern in (a) out from the origin without seeming reference to the graphite re-

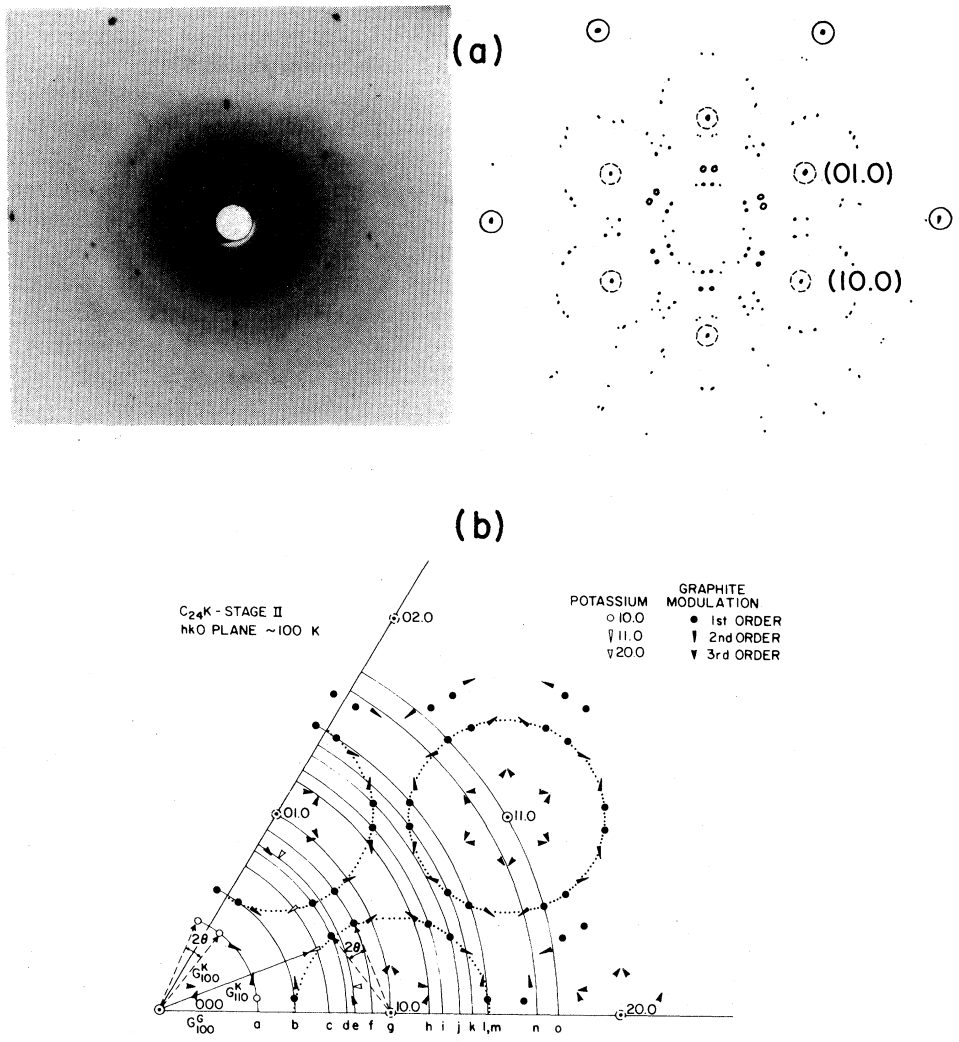


FIG. 1. (a) Transmission x-ray photo of single crystal $C_{24}K$ with Mo$K\alpha$ at ~100 K. The intense diffuse ring comes from the glass holder. In the tracing, the out-of-plane 10.1 and 01.1 are indicated as dotted circles (10.0), (01.0); (11.0) is shown as a closed circle. (b) Schematic interpretation of (a) with HOPG Debye rings indicated as *a*, *b*, *c*, etc., and with the first-order modulation circles indicated.

ciprocal lattice. In other words, the ordered potassium appears to have its own reciprocal lattice—again suggestive of a separate unregistered intercalant structure.[4,7,10] (d) $\lambda/2$ effects coming from the graphite monochromator at positions halfway to the appropriate graphite reflection [with a Ge(111) monochromator, as in Fig. 2, these peaks disappear]. The above features are all present, as well, in Fig. 4 of Parry,[6] including a real $2\times2$ ordered phase accompanying them in $C_{24}Cs$. Parry also shows an intriguing room-temperature pattern of $C_{24}Cs$, recently described, as well by Yamada *et al.*[8] in $C_{24}Rb$, in which the slightly orientationally ordered liquidlike diffuse pattern is reproduced about each graphite relpoint.

Our interpretation of Fig. 1(a) is schematically presented in 1(b). The principal idea behind this figure is the previously stated suggestion that the graphite (*G*) planes bounding or sandwiching a potassium (K) layer are modulated by it. It is, of course, also possible that the graphite remains relatively rigid and modulates the potassium,[7] as with the rare-gas overlayers.[11] If, however, one imposes a small sinusoidal modulation of K on *G* or *G* on

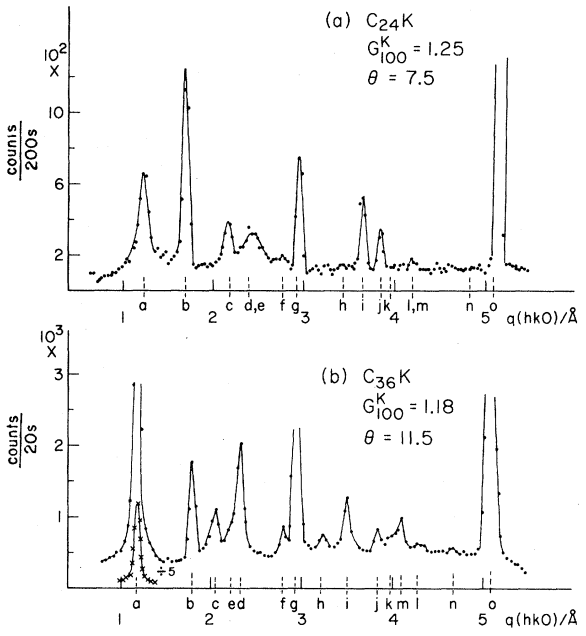


FIG. 2. ($hk0$) scans of HOPG intercalates. (a) $C_{24}K$ (Ref. 2) and (b) $C_{36}K$ at 100 K and 90 K, respectively. (b) was collected with a 12 kW rotating anode supply and graphite monochromator; sample holder was similar to that in Ref. 2.

K, the principal consequences of the two cases are distinguishable as noted in Ref. 10. Imposing a modulation larger than the fundamental period (K modulates $G$) places first-order optical ghosts[13] or sidebands about each $G$ relpoint. Imposing a modulation considerably smaller than the fundamental lattice period ($G$ modulates K) is physically equivalent to a longer wavelength displacement and places first-order sidebands about each K relpoint for which the wave vector must be umklapped back from an outer zone.

Ultimately, however, the argument of which modulates which can only be resolved by intensity measurements since the complete set of allowed ghosts or sidebands of all orders come at $\{\vec{G}^K \pm \vec{G}^G\}$ where $\{\vec{G}^K\}$ and $\{\vec{G}^G\}$ are the set of potassium and graphite reciprocal-lattice vectors, respectively. It is also true that if K pushes on $G$, $G$ must push back, with the important restriction that because the bounding $G$ layers are directly over each other, there can be no component of the modulation of K out of the layer. It should also be understood that if K modulates $G$, there will be satellites about each graphite relpoint for which the diffraction vector ($\vec{K}$) may be approximately normal to the modulation wave vector and thus to the displacement vector ($\vec{u}$) of the (mainly) longitudinal displacement field. If graphite modulates potassium, the diffraction vector is nearly parallel to *all* the modulation vectors. Because in the scattering by lattice displacement waves the intensity $I \propto (\vec{K}\cdot\vec{u})^2$, in the latter case one should expect a fairly uniform intensity variation in the 12 spots about a graphite relpoint. In the former case, one can expect rather dramatic variations about the ring, depending on the rotation angle $\theta$. This fact, noted also by Yamada *et al.*,[8] is an important clue to our qualitative understanding.

We postulate here that the principal features in Fig. 1(a) arise as a consequence of the ordering of the incommensurate or unregistered potassium lattice with stacking $\alpha\beta\gamma/\alpha\beta\gamma$. This lattice has its own Bragg peaks at positions { 10.1 }, { 11.0 }, and { 20.1 }. In addition it modulates the graphite to produce potassiumlike reflections about each graphite reciprocal-lattice point. In Fig. 1(b), the potassium reflections are labeled 10.0, 11.0, 20.0 simply to indicate their positions in the ($hk0$) plane. They and the graphite reflections, of course, obey structure factor rules with the proviso that stacking fault streaking may bring an *hkl* reflection into the ($hk0$) plane.[5] Two potassium wave vectors are labeled $\vec{G}^K_{100}$ and $\vec{G}^K_{110}$, and the rotational separation $2\theta$ is indicated. Potassium peaks beyond 20.1 were not observed, although the sharpness of the first three indicates that a well-defined K lattice exists. In addition it appears that all second-order peaks, including the potassium { 11.0 } and the second-order modulation peaks, lie on the first-order modulation circle about a graphite relpoint. This implies a simple relationship between the lattice periods of K and $G$ and the rotation angle $\theta$, which we will discuss later.

Neglecting for the moment which of the diffraction peaks in Fig. 1(b) occur in the ($hk0$) plane and which occur at a nonzero $l$ index, we may reproduce the peak positions in our earlier $C_{24}K$ (Ref. 2) HOPG pattern by constructing Debye rings about the origin and labeling then $a$, $b$, $c$, $d$, etc. as presented in Fig. 2(a). It is clear that some Bragg peaks (10.1, 11.0, 20.1) arise from a pure potassium lattice while others seem to be essentially pure graphite modulation side bands. The entire set of observed peaks from the HOPG can be indexed in this way, as indicated in Table I.

To illustrate this further we present the low-temperature $C_{36}K$ (stage-III) HOPG pattern in

TABLE I. The indexing of the HOPG diffraction pattern based on Fig. 1(b). $(hk.0)^G_m(1,2,3)$ means (first-, second-, third-) order modulation peak of $hkl$ graphite reflections on $(hk.0)$ plane.

| Index | $(hk.0)$ | $\frac{\lvert G_{hk0}\rvert}{\lvert G^G_{100}\rvert}$ | $q(hk0)$ ($\text{Å}^{-1}$) | HOPG [Fig. 2(a)] | Laue film [Fig. 1(a)] |
|---|---|---|---|---|---|
| $a$ | $(10.0)^K$ | 0.425 | 1.250 | 1.24 | 1.25 |
| $b$ | $(10.0)^G_{m1}$ | 0.581 | 1.709 | 1.70 | 1.74 |
| $c$ | $(11.0)^K$ | 0.736 | 2.165 | 2.18 | 2.22 |
| $d$ | $(10.0)^G_{m1}$ | 0.814 | 2.394 | 2.42 | 2.42 |
| $e$ | $(10.0)^G_{m3}$ | 0.829 | 2.438 | | |
| $f$ | $(10.0)^G_{m1}$ | 0.925 | 2.719 | 2.75 | 2.74 |
| $g$ | $(10.0)^G$ | 1 | 2.94 | 2.94 | 2.99 |
| $h$ | $(10.0)^G_{m2}$ | 1.162 | 3.416 | 3.43 | |
| $i$ | $(10.0)^G_{m1}$ | 1.227 | 3.608 | 3.64 | 3.56 |
| $j$ | $(10.0)^G_{m1}$ | 1.303 | 3.831 | 3.85 | 3.74 |
| $k$ | $(11.0)^G_{m1}$ | 1.349 | 3.967 | | 3.99 |
| $l$ | $(11.0)^G_{m1}$ | 1.419 | 4.171 | 4.19 | |
| $m$ | $(10.0)^G_{m1}$ | 1.422 | 4.182 | | |
| $n$ | $(10.0)^G_{m2}$ | 1.646 | 4.840 | | |
| $o$ | $(11.0)^G$ | 1.732 | 5.092 | | (5.63) |

Fig. 2(b) for comparison. In this case, as at room temperature,[3] $G^K_{100}(\text{III}) < G^K_{100}(\text{II})$. The rotation angle appears to accomodate to the change in potassium-ion size and can be calculated from the HOPG data.[10] The HOPG pattern can then be interpreted in a similar way to $C_{24}K$ and is indexed in Fig. 2(b) (note the reversal of $d$, $e$ and $l$, $m$). We may now assign the ordering peak[2,5] in $C_{24}K$ to the first-order modulation of graphite which vanishes directly with the loss of 3D potassium order. It appears also that the proposed graphite modulation may induce 3D order by stacking the adjacent potassium layers in a pseudocubic close-packed way [see Fig. 3(a)] to minimize the elastic energy.

## III. DIFFRACTION THEORY

To account for the diffraction effects in Figs. 1 and 2, as well as similar observations of other workers on $C_{24}Rb$ (Ref. 7) and $C_{24}Cs$ (Refs. 4 and 6) we have developed a model for the ordered structure in the regime $T_L < T < T_U$ whose model parameters are illustrated in Fig. 3(a). The ensuing diffraction equations are rather complex but the idea is outlined here for clarity:

(1) In a fashion identical to Suzuki *et al.*,[7] we postulate a 3-layer structure for the $c$-axis potassium stacking ($\alpha\beta\gamma$) in each layer of which the potassium forms an unregistered 2D triangular lat-

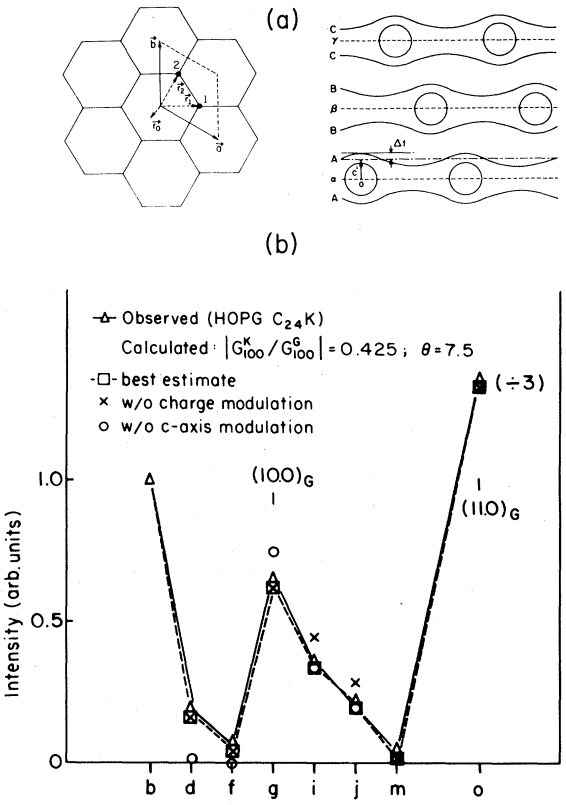


FIG. 3. (a) Left: Model parameters for a modulated graphite plane; Right: the modulation stacking sequence. (b) Relative intensity of several peaks in 2(a) compared with calculations (see text).

tice. The in-plane positions of K atoms in $\beta$ and $\gamma$ layers are related to those of K atoms in the $\alpha$ layer by the fundamental translation vectors $\vec{\Delta}_K=(2\vec{a}_1-\vec{a}_2)/3$ and $\vec{a}_1$ and $\vec{a}_2$ are fundamental vectors of the K layer. $|\vec{\Delta}_K|=5.81$ Å and the in-plane structure of the graphite remains nominally the same as in the original graphite. The in-plane positions of the graphite atoms in the *B* and *C* layers are related to those of the graphite atoms in the *A* layer by the fundamental translation vectors $\vec{\Delta}_G$ and $2\vec{\Delta}_G$ with $\vec{\Delta}_G=(2\vec{b}_1-\vec{b}_2)/3$, $|\vec{\Delta}_G|=2.46$ Å. $\vec{b}_1$ and $\vec{b}_2$ are graphite cell vectors.

(2) The potassium ordering described above within the graphite sandwiches proceeds either via or accompainied by a rotation and an attendant periodic deformation of the graphite.

(3) Along with this periodic lattice modulation of graphite will be a charge readjustment or charge-density wave of the same period. A single charge-density wave (for one potassium reciprocal-lattice vector, $\vec{G}^K$) is of the form

$$\sigma=\sigma_0\cos[\vec{G}^K\cdot(\vec{r}_{ij}+\vec{r}_0)]\ , \tag{1}$$

where $\vec{r}_{ij}$ denotes the *j*th atom of the *i*th graphite cell; $(-\vec{r}_0)$ is the position of the potassium lattice from the center of the 0th cell as in Fig. 3(a).

(4) The magnitude of the expanding of the *i*th cell in our deformation-modulation model is decided by the distance between potassium and the center of the cell. *In other words, each graphite hexagon is deformed by the alkali atom which is attempting to center itself therein.* In this respect our model is different from a simple longitudinal displacement model and represents a point of view midway, so to speak, between an unregistered alkali lattice and a fully registered alkali lattice. The planar static displacement (distortion) wave is evaluated at each of the two atoms of the 2D graphite cell and contains at each the contribution of the three adjacent cells in a single layer. For each atom (1 and 2) we have

$$\begin{aligned}\vec{\Delta}_1=\sum_{\vec{G}^K}\Delta\{&\vec{r}_1\cos[\vec{G}^K\cdot(\vec{r}_i+\vec{r}_0)]+(-\vec{r}_1+\vec{r}_2)\cos[\vec{G}^K\cdot(\vec{r}_i+\vec{a}+\vec{r}_0)]\\&+(-\vec{r}_2)\cos[\vec{G}^K\cdot(\vec{r}_i+\vec{a}+\vec{b}+\vec{r}_0)]\}\ ,\\ \vec{\Delta}_2=\sum_{\vec{G}^K}\Delta\{&\vec{r}_2\cos[\vec{G}^K\cdot(\vec{r}_i+\vec{r}_0)]+(-\vec{r}_1)\cos[\vec{G}^K\cdot(\vec{r}_i+\vec{a}+\vec{b}+\vec{r}_0)]\\&+(\vec{r}_1-\vec{r}_2)\cos[\vec{G}^K\cdot(\vec{r}_i+\vec{b}+\vec{r}_0)]\}\ .\end{aligned} \tag{2}$$

Also,

$$\cos A-\cos B=-2\sin\left[\frac{A+B}{2}\right]\sin\left[\frac{A-B}{2}\right],$$

and therefore,

$$\begin{aligned}\vec{\Delta}_1=&\sum_{\vec{G}^K}\Delta(\vec{r}_1\{\cos[\vec{G}^K\cdot(\vec{r}_i+\vec{r}_0)]-\cos[\vec{G}^K\cdot(\vec{r}_i+\vec{a}+\vec{r}_0)]\}\\&+\vec{r}_2\{\cos[\vec{G}^K\cdot(\vec{r}_i+\vec{a}+\vec{r}_0)]-\cos[\vec{G}^K\cdot(\vec{r}_i+\vec{a}+\vec{b}+\vec{r}_0)]\})\\=&\sum_{\vec{G}^K}2\Delta\left\{\vec{r}_1\sin\tfrac{1}{2}(\vec{G}^K\cdot\vec{a})\sin\left[\vec{G}^K\cdot\left[\vec{r}_i+\vec{r}_0+\frac{\vec{a}}{2}\right]\right]\right.\\&\left.+\vec{r}_2\sin\tfrac{1}{2}(\vec{G}^K\cdot\vec{b})\sin\left[\vec{G}^K\cdot\left[\vec{r}_i+\vec{r}_0+\vec{a}+\frac{\vec{b}}{2}\right]\right]\right\},\end{aligned} \tag{3}$$

i.e.,

$$\vec{\Delta}_1=\sum_{\vec{G}^K}\left\{\vec{d}_1\sin\left[\vec{G}^K\cdot\left[\vec{r}_i+\vec{r}_0+\frac{\vec{a}}{2}\right]\right]+\vec{d}_2\sin\left[\vec{G}^K\cdot\left[\vec{r}_i+\vec{r}_0+\vec{a}+\frac{\vec{b}}{2}\right]\right]\right\}. \tag{4}$$

Similarly,

$$\vec{\Delta}_2=\sum_{\vec{G}^K}\left\{\vec{d}_1\sin\left[\vec{G}^K\cdot\left[\vec{r}_i+\vec{r}_0+\vec{b}+\frac{\vec{a}}{2}\right]\right]+\vec{d}_2\sin\left[\vec{G}^K\cdot\left[\vec{r}_i+\vec{r}_0+\frac{\vec{b}}{2}\right]\right]\right\}.$$

Here

$$\vec{d}_1=2\Delta\vec{r}_1\sin\tfrac{1}{2}(\vec{G}^K\cdot\vec{a}),$$

$$\vec{d}_2=2\Delta\vec{r}_2\sin\tfrac{1}{2}(\vec{G}^K\cdot\vec{b}).$$

$\vec{r}_i$ refers to the $i$th unit cell, $\vec{r}_1$ and $\vec{r}_2$ are basis vectors with components along $\vec{a}$ and $\vec{b}$ of $(\frac{2}{3},\frac{1}{3},0)$ and $(\frac{1}{3},\frac{2}{3},0)$, and $\Delta$ is a displacement amplitude in Å.

(5) Finally, as sketched in Fig. 3(a), we have along [00.$l$] a static displacement wave (transverse to the basal plane):

$$\vec{\Delta}_l=\sum_{\vec{G}^K}\vec{\Delta}_t\cos[\vec{G}^K\cdot(\vec{r}_{ij}+\vec{r}_0)]. \tag{5}$$

Introducing these displacement and charge-density waves into the diffraction equations for the undisturbed $C_{24}K$ and accounting, as noted above, for the stacking of potassium ($\alpha\beta\gamma$) and thus the modulation stacking of graphite requires further simplification to be tractable. This is clear from the fact that we are dealing with a complex set of Bessel funcitons (exponentials of sums over cosine functions). The expressions were therefore simplified through the familiar assumption of small displacements[13] where only the linear term in the expansion of the exponential is kept. If the displacements are large this assumption is bad. Furthermore, the resulting expression will only give reasonable estimates of the intensities of the first-order satellites or ghosts. The higher-order satellite intensities, as pictured in Fig. 2(b), are not calculated properly here even though the derived selection rules for their presence are, of course, correct. The scattered intensity $S(\vec{K})$ is given by

$$S(\vec{K})=\delta(\vec{K}-\vec{G}^G)F_G^2(HKL)+\delta(\vec{K}-\vec{G}^K)F_K^2(MNL)+\delta(\vec{K}-(\vec{G}^K\pm\vec{G}^G))F_M^2(HKLMN),$$

where the $\delta$'s denote the separate Bragg peaks for the $G$ (graphite) lattice, K (potassium) lattice, and $M$ (modulation) lattice. The $F$'s are the structure factors given by

$$F_G(HKL)=8f_G(\vec{K})\cos2\pi L\frac{c'}{c}\cos\frac{\pi}{3}(H-K)[\cos\tfrac{2}{3}\pi(2H+K+L)+\tfrac{1}{2}],$$

$$F_M(HKLMN)=8[\cos\tfrac{2}{3}\pi(2H+K+L+2M+N)+\tfrac{1}{2}]\left[\sigma_0\cos2\pi L\frac{c'}{c}-f_G(\vec{K})\vec{K}\cdot\vec{\Delta}_t\sin2\pi L\frac{c'}{c}\right]\cos\frac{\pi}{3}(H-K)$$

$$-f_G(\vec{K})\vec{K}\cdot\{\vec{d}_1\cos\tfrac{1}{6}[2\pi(H-K)+\vec{G}^K\cdot a+2\vec{G}^K\cdot\vec{b}]$$

$$+\vec{d}_2\cos\tfrac{1}{6}[2\pi(H-K)-2\vec{G}^K\cdot\vec{a}-\vec{G}^K\cdot\vec{b}]\}\cos2\pi L\frac{c'}{c}, \tag{6}$$

$$F_K(MNL)=2\frac{V_G}{V_K}f_K(\vec{K})[\cos\tfrac{2}{3}\pi(2M+N+L)+\tfrac{1}{2}]+F_M(OOLMN).$$

$HKL$ are indices of the graphite reciprocal lattice and $MNL$ are the corresponding potassium indices, $V_G/V_K$ is the unit-cell volume ratio, $c'$ is one-half the graphite plane spacing of those planes with a potassium layer, and $c$ is the $\vec{c}$-axis unit-cell dimension. $F_M(OOLMN)$ is included with $F_K(MNL)$ because in first Brillouin zone the two amplitudes add at the same relpoint. From either Fig. 1 or Fig. 2(a), we have the values for $|\vec{G}^K|=1.25$ Å$^{-1}$ and the angle between $\vec{G}^K$ and $\vec{G}^G$, $\theta=7.5°$.

In Eqs. (6), both $F_G$ and $F_M$ have similar selection rules ($2H+K+L=3M$ or $2H+K+L+2M+N=3m'$) that produce reflections either in the ($hk0$) plane or out at, say, $l=L=\pm1$ ($\pm$ included due to twinning). These predictions have been in detail confirmed with scans in both HOPG and on the single crystal of Fig. 1. For example, peak $a$ is out-of-plane at $l\cong\pm1$, peak $b$ is in-plane ($l\cong0$), $d$ and $f$ are out at $l\cong\pm1$, $i$ and $j$ are in, and $m$ is out ($l\cong\pm1$) as predicted. For detailed comparisons of intensity we have, however, used selected HOPG

data for the graphite peaks (normal and first-order modulation) corrected for powder averaging and polarization and including a careful evaluation of in-plane and out-of-plane effects. This was reluctantly done because the temperature control in the single-crystal experiment was not good enough to guarantee that we were measuring at $T_L < T < T_U$. We have chosen not to fit the potassium reflections although, were we successful, it would afford an important check. There are only three of these [10.1($a$), 11.0($c$), 20.1($e^+$)], and one of them (10.1) has a graphite modulation contribution while another (20.1) is too weak.

Our objective is to account very roughly for the first-order modulation peaks. Because the intensity estimate is uncertain, we are interested only in the rough features of this comparison. For example, modulation peaks $b$ $(100\bar{1}0)$ and $f$ $(10\bar{1}\,\bar{1}1)$ are both first-order satellites about $G^G_{100}$. But $(100\bar{1}0)$ is in-plane while $(10\bar{1}\,\bar{1}1)$ is out at $l \cong -1$. Furthermore, $\vec{K} \sim \| \vec{G}^M_b$ while $\vec{K} \sim \perp \vec{G}^M_f$. The latter fact nearly cancels the structure factor for peak $f$ because the diffraction vector is nearly perpendicular to the largely longitudinal in-plane displacement vector. The sequence of intensity should therefore be $F^2_M(100\bar{1}0) > F^2_M(10\bar{1}\,\bar{1}1)d > F^2_M(10\bar{1}\,\bar{1}1)f$. $d$ and $f$ are the *same* peak merely rotated by $2\theta$. If they have very different intensities, then it is quite likely that the graphite lattice is modulated by the potassium. The displacement field, represented by Eqs. (2)–(4), is not purely longitudinal for which the displacement vector $\vec{u}$ in graphite would be parallel to each modulation wave vector. In fact, were it purely longitudinal, peak $j$ would have to be greater than peak $i$, which it is not. Our cell-expanding model gives the correct variation. If, on the other hand, the graphite modulation of potassium were the principal effect here, the observed variation could not be reproduced for reasons essentially the same as those noted earlier. In addition, if we had solely an amplitude modulation of graphite by alkali which is produced by alkali decoration of graphite hexagons without displacement effects,[12] all pairs of spots about each graphite relpoint would have the same intensity for the two members of each pair.

## IV. RESULTS AND DISCUSSION

The final result for peaks $b$, $d$, $f$, $g$, $i$, $j$, $m$, and $o$ is shown in Fig. 3(b). Our best estimate is $\Delta = -0.06$ Å; $\sigma = -0.108$ electrons; and $|\Delta_t| = 1.5$ Å. Because $\Delta_t$ is so large (it is the amplitude along $\vec{c}$ of the planar modulation), a static attenuation factor was applied to the peak $g$ (the graphite 10.1 or $10.\bar{1}$). This attenuation factor is analogous to a static Debye-Waller factor. Even including the $c$-axis displacements, a value of $\Delta_t = 1.5$ Å is too large—both to be reasonable and to permit the approximation $(\vec{K} \cdot \vec{\Delta}_t) << 1$. In fact, recent single-crystal measurements, both of modulation peaks and 00.$l$ reflections[14] (where the effective attenuation factor has a contribution from the proposed rumpling of the graphite basal planes) suggest that $\Delta_t$ is closer to 0.30 Å.

In summary, certain aspects both of our preliminary fit and the model that motivated it should be emphasized. In the first place, the indexing of all peaks in Fig. 2 and the agreement in Table I are encouraging. The ordered structures of all the Stage-II intercalated materials have proven rather elusive to date, and the intensity and position of the peaks, other than (00.$l$), have yet to be completely accounted for.[8,12] In addition we would note the following:

(1) The charge-density modulation seems to be required although its estimate, based mainly on peaks $i$ and $j$, is uncertain; it is larger by $\sim 2.5$ than the value of the excess charge per layer donated by K ($\sim \frac{1}{2}$ electron per 12 carbon atoms or $\sigma_0 = -0.04$). The charge density buildup in graphite is, as we would expect, between the potassium atom positions, hence the negative value at the potassium site $\sigma_0 = -0.108$.

(2) The in-plane graphite expansion of $\Delta = -0.06$ Å is in phase with the charge buildup; i.e., at the potassium site the graphite axes are contracted.

(3) $\Delta_t > 0$ means, of course, that the graphite is expanded along $c$ at the potassium site and contracted between, as in Fig. 3(a).

(4) A large value of $\Delta_t/\Delta$ is expected from the measured elastic stiffnesses of graphite which control the in-plane ($C_{11}$) and out-of-plane ($C_{44}$) displacements ($C_{11}/C_{44} \approx 300$).[15]

(5) The proposed rumpling or modulation of graphite by the incorporated alkali should be viewed as an inherent tendency of graphite planes (in glassy or polymeric carbon,[16,17] for example) to bend on their own. As in (4) above, graphite is mainly stiff with respect to in-plane stretching.

Finally, returning to the relationship between $\theta$ and atom size, we note that in all cases reported, including $C_{24}Rb$ (Refs. 8, 18, and 19), $C_{24}Cs$ (Ref. 4), and the present $C_{24}K$ and $C_{36}K$, there appears a connection between the rotation angle $\theta$ and the

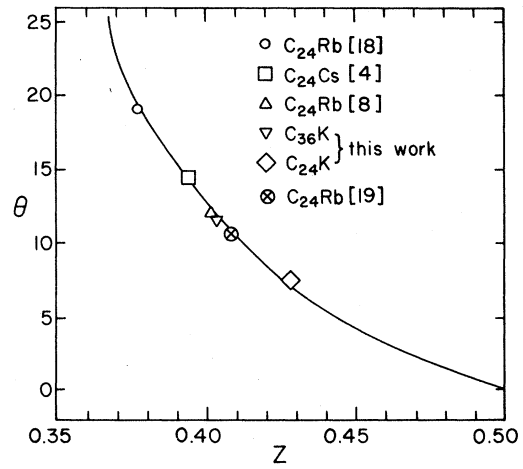


FIG. 4. The rotation angle $\theta$ versus lattice mismatch ratio $z=a_G/a_A$ for several stage-II compounds, where $a_{G,A}$ are in-plane lattice parameters of graphite ($G$) and alkali ($A$). The solid curve is from the expression $\cos(30-\theta)=(2z^2+1)/(2\sqrt{3}z)$.

lattice mismatch ratio $|G^K_{100}/G^G_{100}|=z$. If we require, as appears in Fig. 1(c), that $\vec{G}^K_{110}$ lie always on the modulation "circle" (of radius $|G^K_{100}|$) of about, say, $\vec{G}^G_{100}$, the simple trigonometric relationship follows: $\cos(30-\theta)=(2z^2+1)/(2\sqrt{3}z)$. The above quoted results, plotted in Fig. 4, appear to lie on this curve ($\theta=0$ at $z=0.5$ is the commensurate registry for $2\times2$ structure), permitting a calculation of rotation angle without (initial) regard to the elastic properties of either alkali or graphite. The reported results on $C_{24}Rb$ are noteworthy in that they all lie on the curve although they disagree with each other. This may be due to a temperature dependence of rotation angle[4,8] with, presumably, a concomitant change in $z$. It may also arise from slightly different in-plane concentrations in the three (stage-II) compounds which lead, in these unregistered phases, to different distances of closest approach and thus different values of $z$.

*Note added in proof.* Two additional references have come to our attention which bear comment. The first by Ohnishi and Sugano [Solid State Commun. 36, 823 (1980)] is a calculation of the elastic interaction between intercalant atoms which proceeds through the distortion field in the graphite induced by the intercalant. It is similar in spirit to the work of Safran and Haman [Phys. Rev. Lett. 42, 1410 (1979)] but includes interactions in the $X$-$Z$ plane rather than soley along $Z$ ($c$ axis). The relation to the present problem lies in the importance of the elastic deformation of graphite by intercalated alkali in understanding staging. The second reference is to Clarke, Gray, Homma, and Winokur [Phys. Rev. Lett. 47, 1407 (1981)] in which a model of registered commensurate domains with discommensurations is proposed for the incommensurate ordered state in stage-II alkali intercalates. It is difficult to assess this picture because the position of only a few of the many observed ordering peaks in Ref. 6 are discussed and the intensities are not calculated. It is, however, reasonable to assume that the final (ground) state of an incommensurate structure will involve commensurate registry. How and at what temperature this is achieved remains an open question.

## ACKNOWLEDGMENTS

The U.S. DOE, Division of Basic Energy Sciences, supported M. Mori under Grant No. EY-76-S-05-5111. Y. M. Jan was supported by a joint grant with Michigan State University from the U.S. AROD. The work at Illinois profited from institutional support by the MRL through the U.S. DOE Contract No. CH-1198-028. We thank these organizations. We alos thank S. A. Solin for supplying the crystal and the $C_{36}K$ sample and J. D. Axe for helpful comments.

*Present address: College of General Education, Osaka University, Osaka, Toyonaka, Japan.

[1]G. S. Parry and D. E. Nixon, Nature 216, 909 (1967).
[2]H. Zabel, S. C. Moss, N. Caswell, and S. A. Solin, Phys. Rev. Lett. 43, 2022 (1979).
[3]H. Zabel, Y. M. Jan, and S. C. Moss, Physica (Utrecht) 99B, 453 (1980).
[4]Roy Clarke, N. Caswell, S. A. Solin, and P. M. Horn, Phys. Rev. Lett. 43, 2018 (1979).
[5]J. B. Hastings, W. B. Ellenson, and J. E. Fischer, Phys. Rev. Lett. 42, 1552 (1979).
[6]G. S. Parry, Mater. Sci. Eng. 31, 99 (1977). (Figure 4 and 5 of this paper refer to stage II as suggested by the text.)
[7]M. Suzuki, H. Ikeda, H. Suematsu, Y. Endoh, H. Shiba, and M. T. Hutchings, J. Phys. Soc. Jpn. 49, 671 (1980).
[8]Y. Yamada, I. Naiki, T. Watanabe, T. Kiichi, and H. Suematsu, Physica B (in press); also Y. Yamada, private communication.

[9]D. D. L. Chung, G. Dresselhaus, and M. S. Dresselhaus, Mater. Sci. Eng. 31, 107 (1977).
[10]H. Zabel, in *Ordering in Two Dimensions,* edited by S. K. Sinha (North-Holland, New York, 1980), p. 61.
[11]J. P. McTague and A. D. Novaco, Phys. Rev. B 19, 5299 (1979).
[12]The authors thank Dr. DiCenzo for permission to refer to her unpublished work.
[13]R. W. James, *The Optical Principles of the Diffraction of X-rays* (Bell, London, 1958), pp. 563–571.
[14]Y. M. Jan, thesis for Ph.D., Department of Physics, University of Houston, December, 1980 (unpublished).
[15]R. Nicklow, N. Wakabayashi, and H. G. Smith, Phys. Rev. B 5, 4951 (1972).
[16]G. M. Jenkins and K. Kawamura, *Polymeric Carbons-carbon Fibre, Glass and Char* (Cambridge University Press, New York, 1976), pp. 52–80.
[17]Sumio Iijima, Chem. Scr. 14, 117 (1978–79).
[18]N. Kambe, G. Dresselhaus, and M. S. Dresselhaus, Phys. Rev. B 21, 3491 (1980).
[19]S. C. Moss, K. Liang, W. Warburton, and R. Clarke, unpublished data on HOPG $C_{24}Rb$ taken at the Stanford Synchrotron Radiation Laboratory.

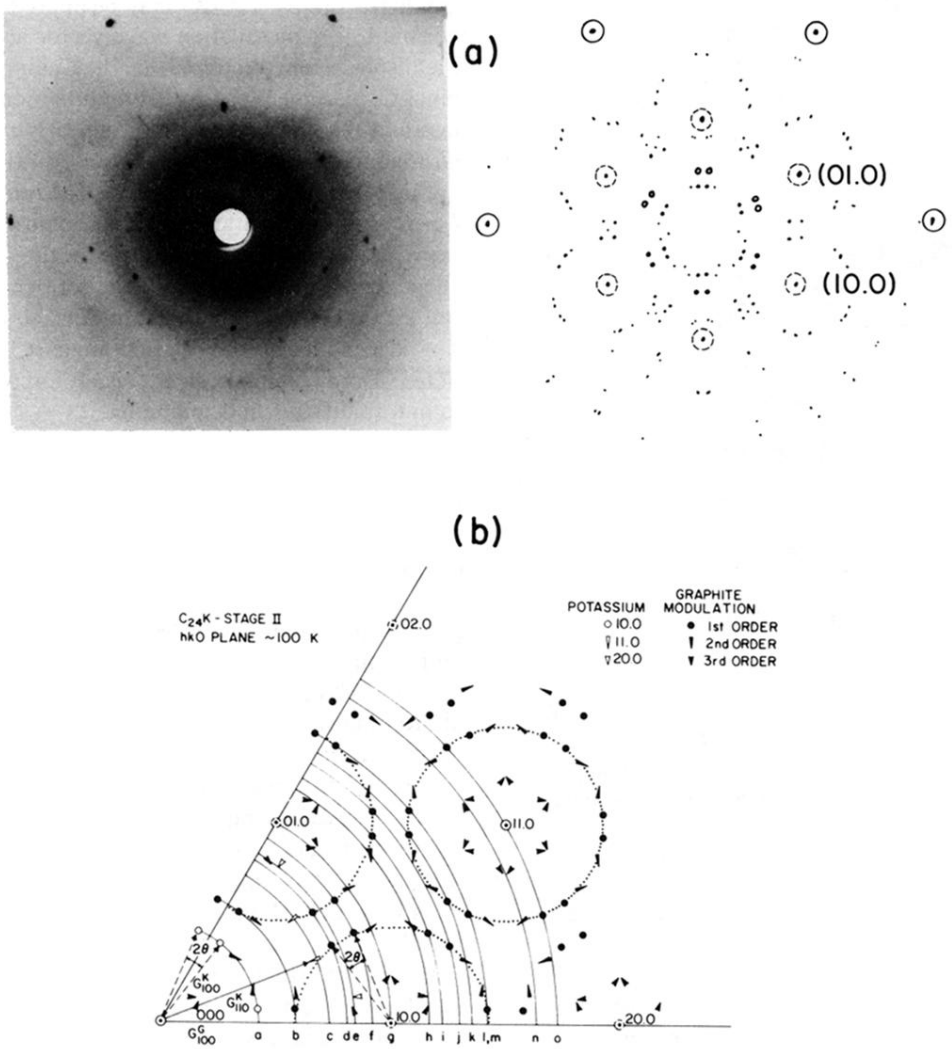


FIG. 1. (a) Transmission x-ray photo of single crystal $C_{24}K$ with Mo $K\alpha$ at $\sim 100$ K. The intense diffuse ring comes from the glass holder. In the tracing, the out-of-plane 10.1 and 01.1 are indicated as dotted circles (10.0), (01.0); (11.0) is shown as a closed circle. (b) Schematic interpretation of (a) with HOPG Debye rings indicated as *a*, *b*, *c*, etc., and with the first-order modulation circles indicated.